10-2013

Rodent herpesvirus Peru encodes a secreted chemokine decoy receptor

Olga Y. Lubman
Washington University School of Medicine in St. Louis

Marina Cella
Washington University School of Medicine in St. Louis

Xinxin Wang
Washington University School of Medicine in St. Louis

Kristen Monte
Washington University School of Medicine in St. Louis

Deborah J. Lenschow
Washington University School of Medicine in St. Louis

See next page for additional authors

Authors

Olga Y. Lubman, Marina Cella, Xinxin Wang, Kristen Monte, Deborah J. Lenschow, Yina H. Huang, and Daved H. Fremont

Journal of Virology

Rodent Herpesvirus Peru Encodes a Secreted Chemokine Decoy Receptor

Olga Y. Lubman, Marina Cella, Xinxin Wang, Kristen Monte, Deborah J. Lenschow, Yina H. Huang and Daved H. Fremont

---

Updated information and services can be found at:
http://jvi.asm.org/content/88/1/538

These include:

REFERENCES
This article cites 52 articles, 28 of which can be accessed free
at: http://jvi.asm.org/content/88/1/538#ref-list-1

CONTENT ALERTS
Receive: RSS Feeds, eTOCs, free email alerts (when new
articles cite this article), more»

Journals.ASM.org

Rodent Herpesvirus Peru Encodes a Secreted Chemokine Decoy Receptor

Olga Y. Lubman,[a] Marina Cella,[a] Xinxin Wang,[a] Kristen Monte,[c] Deborah J. Lenschow,[c] Yina H. Huang,[a*] Daved H. Fremont[a,b]

Departments of Pathology & Immunology,[a] Biochemistry & Molecular Biophysics,[b] and Medicine,[c] Washington University School of Medicine, St. Louis, Missouri, USA

Viruses have long been studied not only for their pathology and associated disease but also as model systems for understanding cellular and immunological processes. Rodent herpesvirus Peru (RHVP) is a recently characterized rhadinovirus related to murine gammaherpesvirus 68 (MHV68) and Kaposi's sarcoma-associated herpesvirus (KSHV) that establishes acute and latent infection in laboratory mice. RHVP encodes numerous unique proteins that we hypothesize might facilitate host immune evasion during infection. We report here that open reading frame (ORF) R17 encodes a high-affinity chemokine binding protein that broadly recognizes human and murine CC and C chemokines. The interaction of R17 with chemokines is generally characterized by rapid association kinetics, and in the case of CCL3, CCL4, CCL5, CCL24, and XCL1, extremely stable complexes are formed. Functionally, R17 potently inhibited CCL2-driven chemotaxis of the human monocytic cell line THP-1, CCL3-driven chemotaxis of peripheral blood mononuclear cells, and CCL2-mediated calcium flux. Our studies also reveal that R17 binds to glycosaminoglycans (GAGs) in a process dependent upon two BBXB motifs and that chemokine and GAG binding can occur simultaneously at distinct sites. Collectively, these studies suggest that R17 may play a role in RHVP immune evasion through the targeted sabotage of chemokine-mediated immune surveillance.

R odent herpesvirus Peru (RHVP) was originally isolated from a lung homogenate of a pygmy rice rat (*Oligoryzomys microtis*) trapped in Peru (1). RHVP can establish latent infection in B6 and 129 mice, with lethal infections observed in mice lacking interferon responses and/or B and T cells (1). The genome of RHVP carries all of the conserved open reading frames (ORFs) found in other rhadinoviruses, such as murine gammaherpesvirus 68 (MHV68) and Kaposi's sarcoma-associated herpesvirus (KSHV), as well as at least 18 unique ORFs that are not broadly conserved among other gammaherpesviruses (1–3). To date, the only functionally characterized protein encoded by RHVP is R12 (pK3), a transmembrane ubiquitin ligase similar to those found in MHV68 and KSHV that downregulates major histocompatibility complex class I (MHC-I) surface expression in a unique manner (4). Sequence analysis of RHVP R5, R6, R7, R17, and R18 is consistent with them encoding secreted, extracellular proteins; all contain leader peptides and lack both transmembrane regions and intracellular localization motifs. Our key hypothesis was that these secreted proteins function to subvert host defense.

Most of the damage inflicted on virally infected cells is the result of activities initiated by proinflammatory cytokines, such as interleukin 1 (IL-1), tumor necrosis factor alpha (TNF-α), and the interferons. Not surprisingly, these and related factors are favorite targets for viral sabotage (5–7). An immune evasion strategy commonly employed by large-DNA viruses is based on the secretion of high-affinity binding proteins that act as cytokine scavengers (8, 9). Frequently, these decoy receptors correspond to soluble versions of their host cellular counterparts. For example, orthopoxviruses encode a secreted protein with ~25% sequence similarity to mammalian gamma interferon (IFN-γ) receptors that binds and functionally inhibits IFN-γ (10, 11). The gammaherpesvirus Epstein-Barr virus (EBV) encodes a secreted decoy that binds colony-stimulating factor 1 (CSF-1), impairing macrophage differentiation, function, and survival (12).

The role of chemokines in orchestrating host defenses is well established, with one hallmark being the establishment of concentration gradients that guide immune responder cells toward sites of infection (13). A wide variety of secreted chemokine binding proteins with the ability to subvert chemokine signaling have been identified, including those encoded by schistosoma parasites, bloodsucking ticks, and herpes- and poxviruses (8, 9). The M3 protein of MHV68 is abundantly secreted during infection and is capable of promiscuously sequestering members of all four chemokine classes with subnanomolar affinities. Functional and structural studies indicate that M3 potently blocks chemokine receptor interactions by competitive inhibition and disrupts chemokine gradients by electrostatically mimicking glycosaminoglycans (GAGs) (14, 15). Other reported herpesvirus proteins that bind chemokines include the human cytomegalovirus (HCMV)-encoded pUL21.5 decoy receptor that has exquisite specificity for human CCL5, binding with high affinity and effectively blocking chemokine receptor activation (16). In contrast to the chemokine decoy receptors encoded by MHV68 and HCMV, the herpes simplex virus 1 (HSV-1)- and HSV-2-encoded gG protein appears to bind chemokines via their GAG binding regions and has been reported to enhance chemotaxis, perhaps to recruit cells pertinent to viral infection or spread (17).

Poxviruses encode a number of distinct chemokine binding proteins. The first group characterized has been termed vCCI (also called M-T1/35k/vCKBP) and refers to abundantly secreted glycoproteins expressed early during viral infection that bind selectively to CC and some CXC chemokines with high affinity (0.03 to 100 nM), blocking their activity (18–21). The second group includes vaccinia A41 and ectromelia E163, which are structurally

similar to vCCI but appear mechanistically distinct. Chemokine mutational analysis was used to demonstrate that A41 binds directly to the GAG recognition regions of chemokines; however, these proteins are ineffective in blocking chemotaxis (22, 23). In addition to blocking chemokine-GAG interactions, E163 itself can tightly associate with GAGs (23). Thus, it appears that these poxvirus proteins may modulate chemokine networks through the disruption of chemokine gradients rather than the competitive inhibition of chemokine receptor binding (22, 23). Although distinct from A41 and E163, myxoma virus encodes M-T7, a secreted glycoprotein that functions both as a species-specific inhibitor of rabbit IFN-γ and as a chemokine binding protein (21). Another group of poxvirus-encoded chemokine binding proteins that have been characterized are termed SECRET domains (24). Chemokine binding studies of the SECRET domains from variola, ectromelia, and cowpox suggest that all of these decoy receptors bind a similar set of chemokines with low nanomolar affinities, including both human and mouse CCL28, CCL25, CXCL12b, CXCL13, and CXCL14 and the mouse chemokines CCL27 and CXCL11. Further, the binding of SECRET domains to the murine chemokine CCL25 was shown to block chemotaxis (24), suggesting that the function of these proteins may be more similar to vCCI discussed above rather than A41 that blocks only chemokine-GAG interactions.

Poxvirus vCCIs are thought to be involved in regulating inflammation during acute infection. Myxoma viruses deficient in M-T1(vCCI) have a subtle phenotype, with an increase in leukocyte infiltration but no significant difference in disease progression or mortality (18, 25). In addition, mouse studies of ORF virus infection, a zoonotic parapoxvirus, shown to encode vCCI-like chemokine binding protein (26), demonstrated that ORF virus (ORFV) vCCI blocks the recruitment of immature and mature dendritic cells to the skin and lymph nodes and inhibits T cell responsiveness in lymph nodes (26, 27). The role of herpesvirus-encoded chemokine binding proteins in pathogenesis and immune modulation remains poorly understood, in part due to lack of the appropriate experimental host. For example, inactivation of M3 expression (by insertion of a translational stop codon) has no apparent consequence on MHV68 infection following intranasal inoculation of C57BL/6 mice (28). Intracerebral injection of the same M3 mutant virus does lead to an altered inflammatory response, with higher numbers of infiltrating lymphocytes and macrophages than observed following inoculation with the wild-type virus (28). However, M3 contributes significantly to MHV68 pathogenesis in a natural host, wood mice, where lack of M3 resulted in substantially reduced latency in the spleen and lung (29, 30).

Despite genetic similarity with MHV68, we have been unable to identify a protein with sequence similarity to the M3 chemokine decoy receptor in the RHVP genome. However, given the recurrence of chemokine binding proteins encoded by diverse large-DNA viruses, we hypothesized that RHVP acquired an alternative approach for disrupting chemokine-induced infiltration of inflammatory cells. Herein, we have examined five secreted proteins encoded by RHVP with the hypothesis that one or more would function as a cytokine decoy receptor. Using cytokine arrays as a screen, we identified R17 as a potential chemokine binding protein. Indeed, R17 binds members of two of the four chemokine families (CC and C), with ligand binding characterized by nanomolar affinities. We show that engagement of chemokines by

R17 blocks their ability to signal through host chemokine receptors and thereby disrupts chemotaxis. We also found that R17 can enhance the association of chemokines with cell surfaces, an observation that we demonstrate is due to the ability of R17 to bind GAGs.

MATERIALS AND METHODS

Ethics statement. Blood from healthy donors was collected at a leukapheresis center and used according to the guidelines of the Washington University Medical Center Human Studies Committee. Peripheral blood mononuclear cells (PBMCs) were isolated using leukoreduction chambers (Trima Accel). This protocol was approved by the Research Ethics Committee and Human Research Protection Office (HRPO) of Washington University, School of Medicine. Since leukoreduction chambers are normally discarded and are stripped of any personal information, the HRPO determined that informed consent was not necessary.

Cloning, expression, and purification of RHVP-encoded proteins. The SignalP 4.1 server predicted the following signal peptide cleavage sites for the secreted proteins of interest: R5 (UnitPro E9M5I4) between Ser 50 and Val 51, R6 (UnitPro E9M5I5) between Gly 22 and Phe 23, R7 (UnitPro E9M5I7) between Ala 18 and Arg 19, R17 (UnitPro E9M5R0) between Cys 27 and Gly 28, and R18 (UnitPro E9M5R1) between Gly 14 and Gln 15. Mature forms of R5, R6, R7, R17, and R18 ORFs without leader peptide were amplified from RHVP virus genomic DNA (accession number NC_015049) and cloned into mammalian expression vector pHLsec (Invitrogen) in frame with the CD33 leader peptide sequence MPLLLLLPL LWAG as either C-terminal Fc fusion or C-terminal 8-His fusion proteins. Fc fusion proteins were used in the Bio-Plex cytokine arrays (Fig. 1). All other assays were performed using R17-His. In this expression vector, the desired gene is under the control of a CMV promoter with a multiple cloning site and an SV40 poly(A) signal. This plasmid carries the origin of replication (oriP) and expresses the EBNA-1 protein from the Epstein-Barr virus that allows long-term episomal maintenance and translocation of the plasmid into the nucleus to enhance protein expression. All constructs were transiently expressed in HEK293F cells in suspension using 293fectin (Invitrogen) as a transfection reagent and grown in Invitrogen's serum-free FreeStyle medium. The culture medium was collected 10 days after transfection, and RHVP-carried ORFs were purified by standard protein A affinity chromatography in accordance with the manufacturer's protocol (GE Healthcare, Piscataway, NJ) and were subsequently buffer exchanged into phosphate-buffered saline (PBS). The R17 C-terminal 8-His fusion construct was purified using Ni-agarose beads (Qiagen, Valencia, CA), followed by size exclusion chromatography (SEC) on a Hi-Load 26/60 Superdex 200 column (GE Healthcare). SDS-PAGE and Western blot analysis confirmed protein purity. Two additional variants of R17 were used in this study: R17 mutant, where residues 29 to 32 of the mature sequence RKDR (BBXB) were mutated to EDDE and are referred to as $R17^{GAG1}$ and residues 333 to 337 of the mature sequence KGRRK (BXBBB) were mutated to DGEED and are referred to as $R17^{GAG2}$. Mutagenesis was performed using a multisite QuickChange mutagenesis kit (Agilent Technologies) on the background of the wild-type R17 C-terminal His construct and verified by DNA sequencing. The identity of R17 was confirmed by N-terminal sequencing (Midwest Analytical, Saint Louis, MO).

Bio-Plex cytokine arrays. Customized Bio-Plex pro arrays (Bio-Rad) were ordered to detect murine IL-6, IL-1β, IL-10, IL-12p70, IL-13, IFN-γ, CCL2, CCL3, CCL5, and TNF-α. The assay was run per the manufacturer's guidelines, with the exception that recombinant RHVP Fc fusion proteins were preincubated with the recombinant standards for 20 min prior to the addition to the assay plate. In brief, the antibody-coupled beads of the 10 analytes were prepared in assay buffer and then placed in each well of the assay plate. The recombinant standards were diluted as outlined in the manufacturer's guidelines, and the standard was then diluted 1:3 to generate a standard curve. After the standards were diluted, 150 μl of PBS, R17-Fc, or R6-Fc was added to each of the standards and incubated for 20 min at room temperature. The standards were then added to each well and
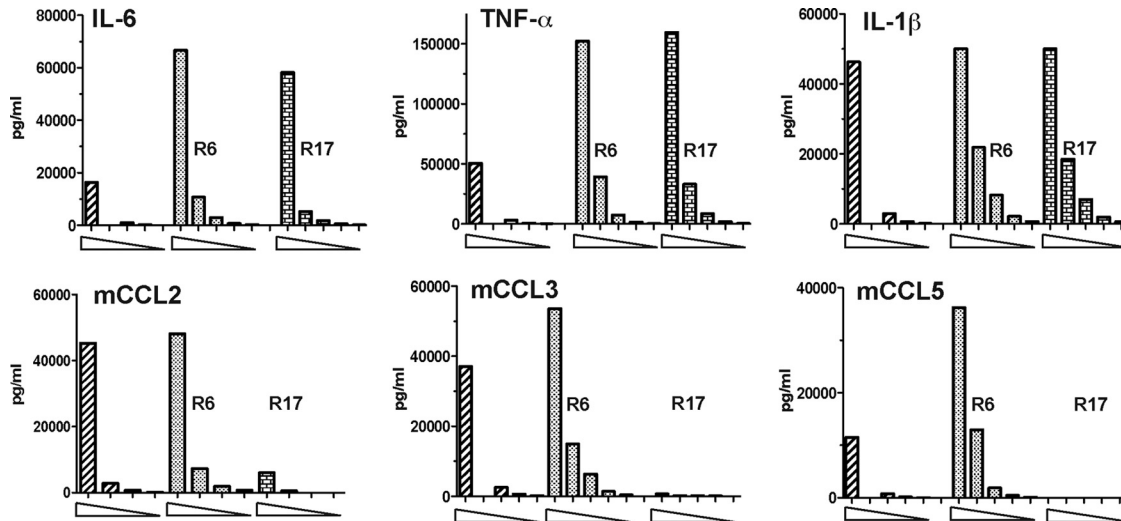
FIG 1 R17 pages interaction of chemokines with specific antibodies. Purified R17 (1 μM) and purified R6 (1 μM) were preincubated with serial dilutions of recombinant cytokine standards prior to the addition to a Bio-Plex plate. The recombinant standards were diluted as outlined in the manufacturer's guidelines, and the standard was then diluted 1:3 to generate a standard curve. R17 inhibited the detection of mCCL2, mCCL3, and mCCL5 by chemokine-specific antibodies but had no effect on the interaction of IL-6, TNF-α, or IL-1β with their cognate antibodies.

incubated on a shaker at room temperature for 30 min. The plate was washed 3 times, and then detection antibody was added and incubated on a shaker for 30 min at room temperature. The plate was again washed 3 times, and then streptavidin-PE was added to each well and incubated on a shaker at room temperature for 10 min. After the plate was washed 3 times, 125 μl of assay buffer was added to each well, and the plate was read on a Bio-Plex plate reader system using Bio-Plex Manager software for analysis.

Recombinant chemokines. Murine CCL2 and CCL3 chemokines were expressed in *Escherichia coli*, refolded from inclusion bodies, and purified as previously described (31). All chemokines except for murine CCL2 and CCL3 were purchased from Peprotech. Biotinylation of chemokines was performed using EZ-Link *N*-hydroxysuccinimide (NHS)–polyethylene glycol 4 (PEG4)–biotin (Thermo Scientific) using a 2:1 molar ratio of biotin to chemokines. Unbound biotin was removed using Thermo Scientific Zebra spin desalting columns per the manufacturer's instruction.

SPR binding analysis. Surface plasmon binding (SPR) was used to directly measure the affinity and kinetics of chemokine binding by R17 and its variants. R17, R17^{GAG1}, and R17^{GAG2} were immobilized on a CM5 chip (GE Healthcare) using standard amine coupling chemistry (Biacore amine coupling kit) to a level of 200 to 500 response units (RU) for kinetic binding analysis and 1,000 RU for equilibrium binding analysis using a Biacore T-100 biosensor (GE Healthcare). A control flow cell was prepared by coupling non-chemokine binding protein R7 or NeutrAvidin to the chip at a similar level. Experiments were performed at 100 μl/min and 25°C using HBS-EP (10 mM HEPES [pH 7.5], 150 mM NaCl, 3 mM EDTA, 0.005% Tween 20) as a running buffer. High flow rates and low levels of coupled proteins were used to minimize the effects of mass transport. For all kinetic experiments, 358 μl of chemokine was injected over experimental and control flow cells followed by a 500-s period to monitor dissociation before regeneration was achieved by injecting 100 μl of 0.1 M glycine (pH 2.0). Each experiment was performed at a minimum of three times with eight different chemokine concentrations followed by three buffer injections. The association (K_a) and the dissociation (K_d) values were determined simultaneously by globally fitting sensograms for an entire range of chemokine concentrations to a 1:1 mass transport model with BIAevaluation software. This global analysis was performed independently for each series of concentrations, the resulting values were averaged, and the standard deviation was calculated to reflect the experimental error. Apparent equilibrium dissociation constants were

determined either from the kinetic values using the equation $K_{D,kin} = K_d/K_a$ or from saturation binding experiments, $K_{D,eq} = $ RU response/chemokine concentration.

Chemotaxis assay. THP-1 cells were cultured in RPMI 1640 medium supplemented with 10% fetal bovine serum (FBS), 1 mM sodium pyruvate, 100 units/ml penicillin, 100 μg/ml streptomycin, and 2 mM L-glutamine. Cell culture was maintained between 2×10^5 and 9×10^5 cells/ml at 37°C with 5% CO_2. PBMCs were isolated from heparinized blood by Ficoll gradient centrifugation (GE Biosciences) and resuspended in RPMI 1640 medium supplemented with 1% bovine serum albumin (BSA). Ninety-six-well Transwell permeable support inserts (Corning Costar; Sigma-Aldrich) were used. Human CCL2 and CCL3 at concentrations of 10 nM were diluted in 1% BSA RPMI and placed in the lower compartment, and 6×10^4 of either human THP-1 monocytes or 1×10^5 human PBMCs were placed in the upper chamber, separated by a 5-μm-pore-size filter. After PBMCs were incubated for 3 h and the THP-1 cells for 4 h at 37°C, the cells in the lower chamber were spun, lysed, and counted using CyQuant dye (Life Technologies). For competition experiments, three proteins, R17, M3, and R7, were added to the lower chamber to a final concentration of 100 nM. The bacterially refolded purified M3 was used as a positive control for inhibition, while R7 was used as a negative control for inhibition.

Calcium mobilization assays. THP-1 cells were incubated at a density of 5×10^6 cells/ml in Ca^{2+} buffer with 1 μM Fura-2AM loading dye and 0.02% pluronic at 37°C for 30 min in the dark before being washed twice and resuspended at 5×10^6 cells/ml in Ca^{2+}-free buffer. Fura-2-loaded cells were transferred into a poly-L-lysine-treated 96-well assay plate at 5×10^5 cells/well for CCL2 stimulation. A total of 160 nM CCL2 was preincubated with buffer control, 2 μM R17, 2 μM MR1 (32), or 1 μM M3 for 5 min at 37°C prior to cell stimulation. Ca^{2+} response was measured on a FlexStation system from Molecular Devices based on the spectrofluorimetry at 37°C.

Competition of chemokine binding to cells. To evaluate CCL2, CCL3, and CCL5 binding to CHOK1 and CHO745 cells, chemokines and a negative-control protein (MR1) (32) were nonspecifically biotinylated using the EZ-biotin kit (Pierce) using a 2:1 biotin-to-protein molar ratio, followed by removal of unbound biotin (Thermo Scientific Zebra desalting columns). CHOK1 and CHO745 cells were maintained in F-12 medium supplemented with 10% fetal calf serum (FCS) and 100× Penn-Strep. On the day of the experiment, cells were washed once with PBS,
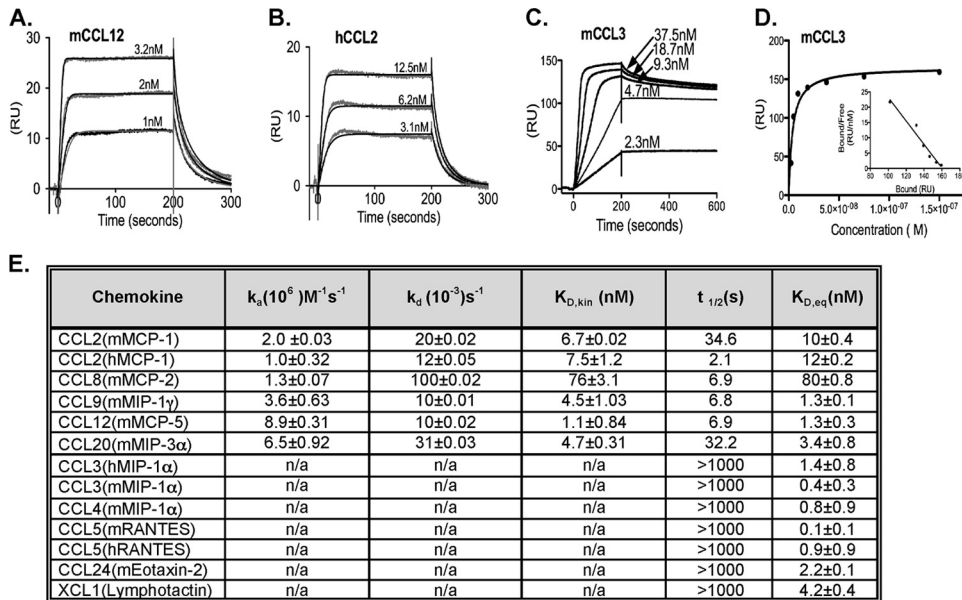
FIG 2 R17 binds CC and C chemokines with high affinity. (A and B) SPR sensograms of mCCL12 and hCCL2 binding to CM5 chip immobilized R17. The experimental curves (gray lines) are globally fit using a 1:1 mass transport model (black lines) to determine kinetic parameters. (C) Shown is a representative response curve for the saturation binding analysis of mCCL3 to R17, which cannot be accurately globally fit. (D) Saturation curve and Scatchard plot for the binding of mCCL3 to R17. (E) Tabulation of the interaction parameters for human and murine chemokines binding to R17. Reported values for K_a, K_d, and $K_{D,kin} = K_d/K_a$ are derived from globally fit binding analysis as means ± standard deviations. Reported values for $K_{D,eq}$ are derived from Scatchard analysis of the saturation binding analysis as means ± standard deviations. The following cytokines were tested, and no binding was observed under the same experimental conditions: mCCL21, mCXCL8, mCXCL10, mCXCL9, mCXCL2, mCXCL12, mCXCL1, CX3C, mIL-13, mIL-12, mIL-6, mIL-17, mTNF-α.

detached using 0.2% EDTA, and resuspended in staining buffer containing PBS, 0.5% BSA, and 2 mM EDTA. Biotinylated chemokines were added to cells to a final concentration ranging from 50 to 250 nM, incubated for an hour on ice, washed twice, and detected with streptavidin PE (Life Technologies) using flow cytometry. To determine the effect of R17, R17^{GAG1}, and R17^{GAG2} on CCL2-, CCL3-, and CCL5-GAG interaction, 0.1 to 0.5 μM of R17 or R17^{GAG1} or R17^{GAG2} was precomplexed with biotinylated chemokines and incubated with both CHOK1 and CHO745 cells. As a positive control for inhibition, bacterially refolded M3 was used. Flow cytometry was undertaken using a FACS array or FACSCalibur, and data were analyzed using FlowJo software.

R17 binding to cells. R17, R17^{GAG1}, and R17^{GAG2} were nonspecifically biotinylated using the EZ-biotin kit (Pierce) using a 2:1 biotin-to-protein molar ratio, followed by removal of unbound biotin (Thermo Scientific Zebra desalting columns), and added to CHOK1 and CHO745 to a final concentration of 0.2 μM in the same manner as described in the section above.

RESULTS

Production of five secreted proteins uniquely encoded by RHVP. We began our studies of RHVP by examining the genome for the presence of novel ORFs encoding proteins that may be secreted during viral infection. Five hypothetical proteins were identified that contain an N-terminal signal peptide but lack any apparent transmembrane regions or intracellular retention motifs (R5, R6, R7, R17, and R18). Analysis of these RHVP protein sequences using the fold recognition server PHYRE2 (33) indicates that R5, R7, and R18 likely are all composed of four tandem Ig domains, while positively charged R6 might fold as a helical bundle. The sequence of R17 produced no significant hits using this analysis, although we note that the protein is predicted to have a low isoelectric point (pI = 5.7), a common feature among previously identified chemokine binding proteins (15, 20). The mature

sequences of all five ORFs were amplified from RHVP genomic DNA (with endogenous signal peptides removed) and cloned into the mammalian expression vector pHLsec in frame with the CD33 signal peptide as either C-terminal Fc or His tag fusion proteins. Constructs were transiently expressed in HEK293F cells, and the secreted RHVP proteins were purified by standard chromatography methods.

Screening of cytokine binding by RHVP-encoded proteins. Our initial approach toward identifying functions for R5, R6, R7, R17, and R18 involved screening of a panel of cytokines using Bio-Plex cytokine arrays (Bio-Rad). These arrays were originally designed to test for the presence of cytokines in cell culture medium using cytokine-specific antibodies (34). In our experiments, soluble RHVP Fc fusion proteins (1 μM) were premixed with select murine cytokine standards, and competition with the bead-coupled detection antibodies was assessed. As seen in Fig. 1, serial dilution of IL-6, TNF-α, or IL-1β in the presence of either R6 or R17 did not affect the cytokine-antibody interaction. However, serial dilutions of CCL2, CCL3, or CCL5 in the presence of R17 but not in the presence of R6 inhibited the ability of these chemokines to bind their respective antibodies (Fig. 1). Fc fusion proteins of R5, R7, and R18 also did not disrupt chemokine-antibody interactions, and none of the examined RHVP proteins appeared to block specific antibody detection of IL-10, IL-12p70, IL-13, or IFN-γ (data not shown). Thus, the Bio-Plex screen uniquely identified RHVP R17 as a potential chemokine binding protein.

R17 binds CC and C family chemokines with high affinity. To assess the ability of R17 to directly interact with chemokines, we have screened a large panel of different chemokines and cytokines using surface plasmon resonance (SPR) (Fig. 2). In these experiments, R17 was covalently coupled to a BIAcore CM5 chip and
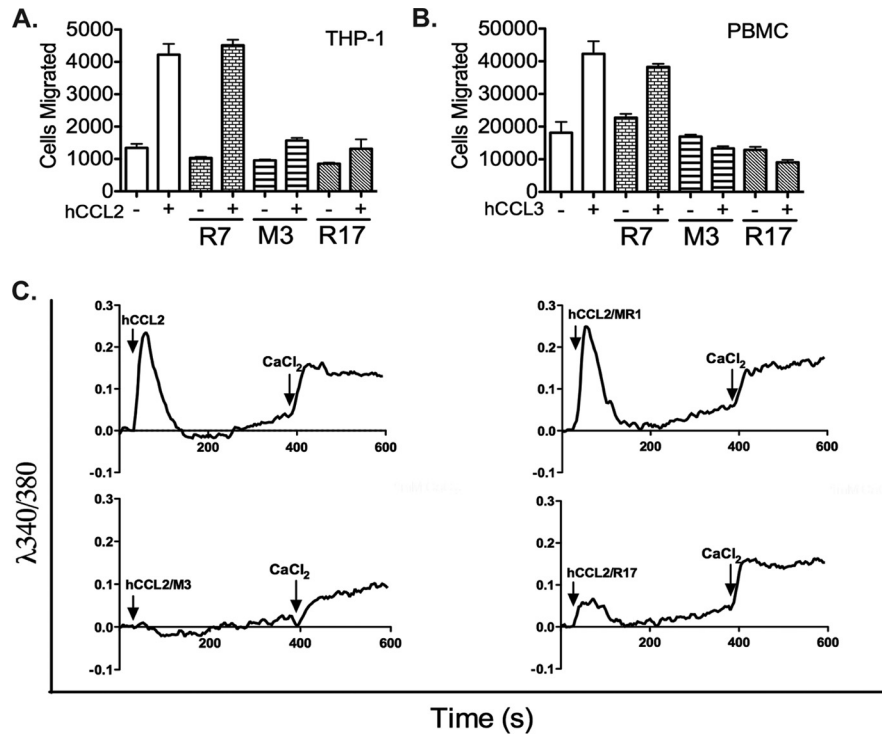
FIG 3 R17 blocks CC chemokine-mediated transmigration and receptor signaling. Transmigration of either THP-1 cells stimulated with hCCL2 (A) or human PBMCs stimulated with CCL3 (B) in the presence and absence of R17, M3 (positive control), and R7 (negative control). Different complexes were formed by incubating 10 nM hCCL2 with 100 nM R7, M3, or R17 at room temperature for 30 min and added to the bottom of a transmigration plate. A total of 6×10^4 THP-1 cells or 1×10^5 PBMCs were added to the top of Transwell inserts. The transmigration plates were incubated at 37°C for 4 h for THP-1 chemotaxis and 3 h for PBMC chemotaxis. The cells that migrated from the Transwell insert to the bottom of transmigration plates were pelleted and counted using CyQuant dye. Standard deviations represent averages from at least three independent experiments. (C) Shown are the changes in relative fluorescence of Fura-2-loaded cells (ratio of $\lambda 340$ to $\lambda 380$), which monitors the intracellular Ca^{2+} concentrations. THP-1 cells were stimulated for 30 s with hCCL2 (160 nM) either alone or in complex with the following proteins: negative-control MR1 (2 μM), positive-control M3 (1 μM), and R17 (2 μM). Ca^{2+} flux from the endoplasmic reticulum (ER) was measured for 400 s, followed by the addition of 1 mM Ca^{2+} to measure influx. Data are representative of at least three separate experiments.

examined for specific ligand binding. C-terminal Fc or His was not used for immobilization, because highly charged chemokines nonspecifically interact with antibodies necessary to capture proteins either by Fc or His tag. Of the 25 mouse and human chemokines tested, a concentration-dependent increase in the refractive index together with saturable binding was observed for mCCL2 and hCCL2, for mCCL3 and hCCL3, for mCCL4, mCCL5 and hCCL5, and for mCCL8, mCCL11, mCCL20, mCCL24, mCCL19, mCCL12, and mXCL1. As negative controls for chemokine binding, we used either a NeutrAvidin-coupled chip or RHVP R7; both of these proteins lack chemokine binding activity. From the SPR experiments, we have determined that R17 directly interacts with all of the CC chemokines we tested except mCCL21, a chemokine expressed constitutively in secondary lymphoid tissues and thought to be essential for cell migration into lymphoid organs (35, 36). We have also determined that R17 binds the C chemokine lymphotactin (XCL1). In contrast, R17 did not interact with any of the CXC chemokines we examined (mCXCL8, mCXCL10, mCXCL9, mCXCL2, mCXCL12, mCXCL1) or the CX3C chemokine fractalkine. SPR binding studies with other murine cytokines (IL-13, IL-12, IL-6, IL-17, TNF-α) did not reveal any additional R17 ligand binding specificities. Among the chemokines that R17 binds, the apparent complex half-lives ($t_{1/2}$) vary considerably. For example, mouse and human versions of CCL2, CCL9, CCL12, and CCL20 all form complexes with measurable off rates ($t_{1/2}$

varying from 2 to 32 s), and we report in Fig. 2E equilibrium and kinetic binding parameters which generally are in agreement. In contrast, CCL3, CCL4, CCL5, and XCL1 form stable complexes with extremely slow dissociation rates that appear to be in excess of 10 min (Fig. 2). Quantitative kinetic characterization of the latter chemokines could not be measured accurately due to mass transport limitations during the association phase and lack of an appropriate competitor to speed up the dissociation phase. We therefore report apparent $K_{D,eq}$ values determined from saturation binding analysis for these chemokines (0.1 to 4 nM), although the actual affinities may well be picomolar.

R17 blocks chemokine-mediated cell migration. Based on the known mechanisms of viral immune evasion, we hypothesized that R17 may function as a viral decoy that prevents chemokine recruitment of immune cells to sites of infection (8). To address the functional consequences of R17-chemokine interactions, we performed experiments evaluating the migration of the human monocytic cell line THP-1 in response to hCCL2, a fast dissociating R17 ligand ($K_{D,eq} = 12$ nM, $t_{1/2} = 2.1$ s), and human PBMCs in response to hCCL3, a slow off-rate R17 ligand ($K_{D,eq} = 1.4$ nM, $t_{1/2,app} > 1,000$ s). We found that R17 potently blocked THP-1 cell transmigration when incubated in 10-fold molar excess of CCL2 (Fig. 3A). Similar disruption was observed when we incubated CCL2 with the M3 decoy receptor encoded by MHV68, which was previously shown to effectively block cell migration mediated by
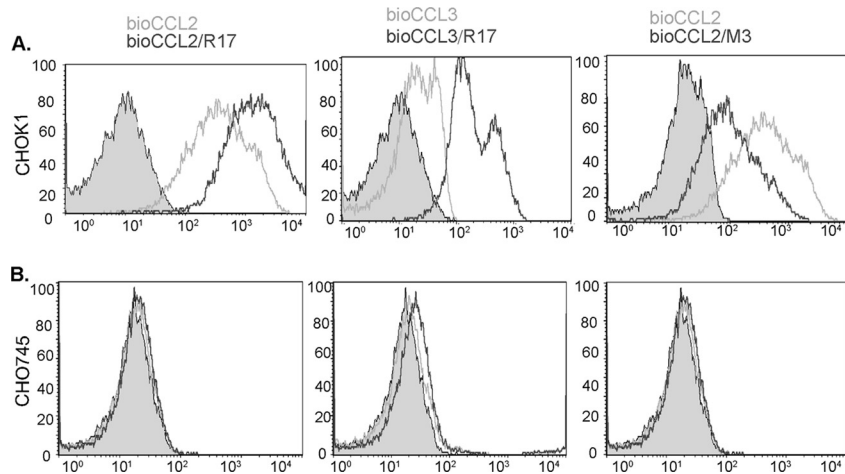
FIG 4 R17 enhances chemokine cell surface binding. Flow cytometry analysis of CHOK1 (A) and CHO745 (GAG-deficient) (B) cells stained by 10 nM biotinylated mCCL2 and mCCL3 in the presence or absence of either 100 nM R17 or 100 nM M3.

CCL19 and CCL21 (37). As a negative control, we used RHVP R7 that lacks chemokine binding activity. Similar results were obtained when we examined the ability of R17 to disrupt CCL3-mediated transmigration of human PBMCs, where R17 and M3 proved inhibitory while R7 did not (Fig. 3B).

R17 blocks chemokine-mediated calcium release. Activation of chemokine receptor signaling leads to calcium release from endoplasmic reticulum stores resulting in elevated levels of cytoplasmic calcium (38). Changes in calcium levels upon chemokine stimulation can be monitored in real time by Fura-2 dye-loaded cells. Previous experiments with MHV68 M3 revealed that it is an effective Ca^{2+} flux inhibitor for several distinct chemokines that it engages (39). We have tested the ability of R17 to inhibit transient increase in intracellular calcium induced by hCCL2 in THP-1 cells. When added in 10-fold molar excess, R17 effectively diminishes CCL2-mediated calcium flux, albeit not as effectively as M3, which forms significantly more stable complexes with CCL2 (Fig. 3C). The addition of a negative-control protein, MR-1 (32), showed no changes in CCL2-mediated calcium mobilization. Together with the transmigration assays, these data suggest that R17 might function as an inhibitor of CC chemokine signaling.

R17 interacts with cell surface GAGs. To function properly, chemokines need to interact with their cognate G protein-coupled receptor as well as glycosaminoglycans (GAGs) on extracellular surfaces where they establish their gradients (9, 40). The viral chemokine binding proteins described to date have been shown to interfere with chemokine-GPCR interactions, chemokine-GAG interactions, or both (8). To assess the ability of R17 to block chemokine-GAG interactions, we conducted cell surface binding and competition assays. CHOK1 cells, rich in heparan and chondroitin sulfates, are readily stained with randomly biotinylated CCL2 and CCL3, while the analogous flow cytometry experiments carried out using the GAG-deficient CHO745 cell line (41) result in minimal background staining (Fig. 4). As we previously reported, M3 was effective in blocking the interaction between CCL2 and cell surface GAGs (Fig. 4) (15). It is important to note that complete inhibition of CCL2-GAG interactions by M3 was evident when a BirA-tagged version of CCL2 was used in contrast to the randomly biotinylated CCL2 used in the experiments described here (15).

Surprisingly, when we preincubated biotinylated CCL2 or CCL3 with a 5-fold molar excess of R17, we observed a dramatic increase in chemokine staining of CHOK1 but not CHO745 cells (Fig. 4). To address a potential mechanism through which R17 was able to enhance chemokine cell staining, we examined the ability of biotinylated R17 alone to stain CHOK1 and CHO745 cells. We discovered that biotinylated R17 readily stains CHOK1 but not CHO745 cells, suggesting that R17 specifically interacts with cell surface GAGs (Fig. 5). This result not only identified an additional binding partner for R17 but also enabled a clearer interpretation of the enhanced chemokine cell staining mediated by R17. We propose that because R17 engages both chemokines and cell surface GAGs, it is able to trap chemokines at the cell surface, resulting in our observed increase in CHOK1 staining by biotinylated CCL2 and CCL3.

R17 interacts with GAGs via determinants distinct from chemokine binding. Our flow cytometry experiments suggest that R17 can simultaneously engage cell surface GAGs and chemokines. Examination of the amino acid sequence of R17 reveals the presence of two BBXB motifs known to be important for GAG binding in a number of different proteins (42, 43). We therefore created two variants of R17 through site-directed mutagenesis, R17^{GAG1}, in which residues 29 to 32 RK_DR (BBXB) were mutated to ED_DE, and R17^{GAG2}, where residues 333 to 337 KG_RRK (BXBBB) were mutated to DG_EED. When tested, neither biotinylated R17 variant was capable of staining CHOK1 cells, suggesting that both BBXB motifs are indeed critical for GAG binding (Fig. 5A). However, both R17^{GAG1} and R17^{GAG2} bound CCL2 and CCL3 with binding parameters comparable to those observed for wild-type R17 (Fig. 5B). Thus, the R17 determinants for cell surface GAG binding are distinct from those mediating the high-affinity binding of CC chemokines.

DISCUSSION

Here, we describe the identification and characterization of a novel soluble chemokine binding protein, R17, encoded by RHVP. The mature secreted R17 protein is composed of 412 residues with six potential disulfide bridges and three Asn-linked glycosylation sites. R17 displays no appreciable amino acid sequence similarity to any other viral or cellular protein. In contrast
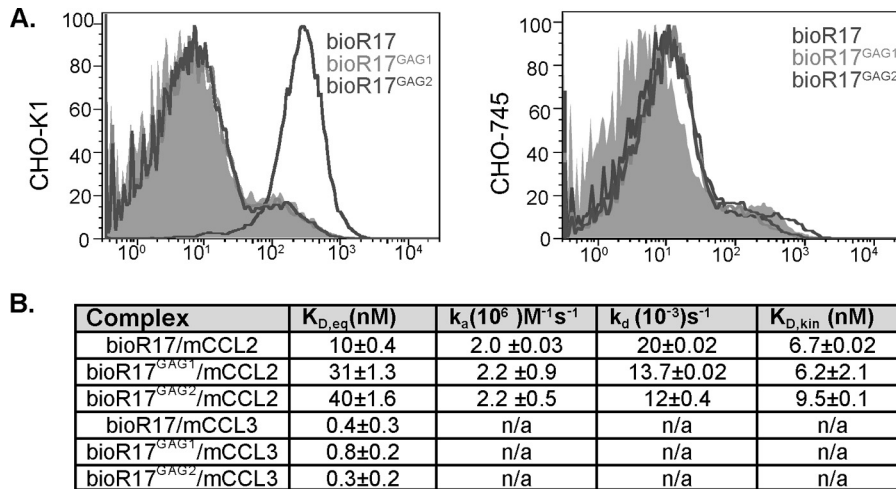
B.

Complex	$K_{D,eq}$ (nM)	$k_a (10^6) M^{-1}s^{-1}$	$k_d (10^{-3})s^{-1}$	$K_{D,kin}$ (nM)
bioR17/mCCL2	10±0.4	2.0 ±0.03	20±0.02	6.7±0.02
bioR17^{GAG1}/mCCL2	31±1.3	2.2 ±0.9	13.7±0.02	6.2±2.1
bioR17^{GAG2}/mCCL2	40±1.6	2.2 ±0.5	12±0.4	9.5±0.1
bioR17/mCCL3	0.4±0.3	n/a	n/a	n/a
bioR17^{GAG1}/mCCL3	0.8±0.2	n/a	n/a	n/a
bioR17^{GAG2}/mCCL3	0.3±0.2	n/a	n/a	n/a

FIG 5 R17 interacts with cell surface GAGs at a site distinct from chemokine binding. (A) Flow cytometry analysis of CHOK1 and CHO745 cells stained by biotinylated R17 and the BBXB mutants R17^{GAG1} and R17^{GAG2}. (B) SPR binding analysis of the interaction of CCL2 and CCL3 with R17^{GAG1} and R17^{GAG2}.

to the highly promiscuous chemokine binding of MHV68 M3 (39), R17 binds selectively to CC chemokines and XCL1. Our SPR studies indicate that R17 binds CCL2, CCL8, CCL9, and CCL20 with affinities ranging from 1 to 80 nM, rapid association kinetics, and half-lives of 2 to 35 s. R17 engages another group of chemokines (CCL3, CCL4, CCL5, CCL24, and XCL1) with extremely long half-lives that are difficult to quantitate but we estimate as greater than 10 min. As such, the chemokine binding properties of R17 closely resemble those of the vCCI decoy receptor encoded by ectromelia, EVM1, which forms moderately fast dissociating complexes with CCL2 and highly kinetically stable complexes with CCL3 and CCL5 (20). The difference in the off rates among two groups of R17-chemokine complexes is interesting and is likely to reflect variation in specific amino acids important for this interaction. For example, structural inspection of CCL2, CCL3, and CCL5 chemokines together with mutagenesis data indicate distinct positioning of basic residues thought to mediate GAG binding. While CCL3 and CCL5 have BBXB motifs localized to the 40's loop (loop connecting beta strands 2 and 3), GAG binding residues on CCL2 have been mapped to R18, K19, and R24 of the N-terminal loop (20's loop) (44).

Similarly to MHV68 M3 and poxvirus vCCIs, RHVP R17 appears to operate as a true decoy receptor, blocking the ability of chemokines to activate their host receptors (Fig. 6). Our data indicate that R17 capably inhibits both CCL2- and CCL3-driven transmigration despite the fact that CCL3 is a much tighter binder. But our comparison of the abilities of R17 and M3 to block CCL2-mediated calcium release indicates a greater potency for M3, which binds this chemokine with a significantly longer half-life than R17.

In addition to chemokine binding, R17 also tightly associates with cell surface GAGs. Indeed, our flow cytometry experiments indicate that R17 can dramatically increase the association of chemokines with cell surfaces. We inspected the primary sequence of R17, finding two basic BBXB motifs that are commonly found in GAG binding proteins, including many chemokines. R17 variants lacking either BBXB motif do not bind cell surface GAGs, and chemokine binding experiments with these variants indicate that the R17 chemokine and GAG binding sites are independently po-

sitioned. As such, the increased chemokine cell surface association we observed can be explained by the high-affinity binding of chemokines to GAG-associated R17. In this regard, R17 exhibits similarity with myxoma virus MT-1 (vCCI) that has been shown to interact with cell surface GAGs while simultaneously blocking receptor-mediated chemokine signaling (45). In contrast, ectromelia E163 binds both chemokines and GAGs, although unlike R17 and MT-1, disruption of chemokine signaling by this protein has not been observed (23).

The idea of using virally encoded decoy receptors to therapeutically block chemokine signaling was introduced a few years ago (46). For example, vCCI has been shown to diminish inflamma-
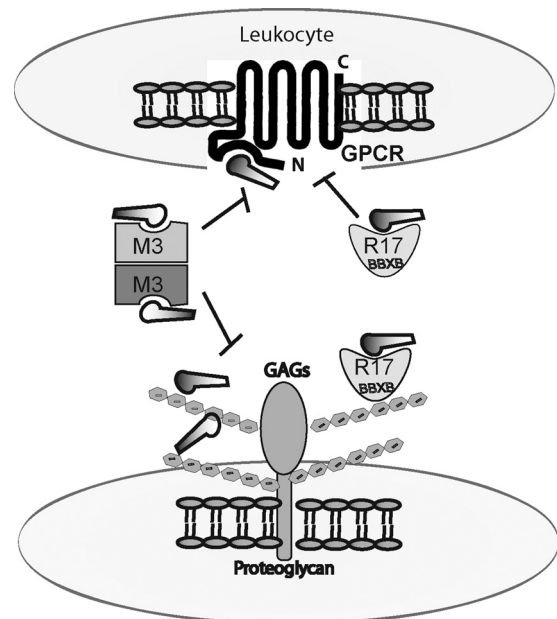

FIG 6 Sabotage of chemokine function by R17 and M3. Schematic diagram illustrating R17- and M3-mediated disruption of chemokine binding to GPCRs, M3-mediated disruption of chemokine-GAG interactions, and R17 association with cell surface GAGs.

tion in allergen-induced asthma (47) and intraperitoneal injection mouse models (48). MT-1 treatment was shown to alleviate vascular pathology by inhibiting early monocyte and lymphocyte infiltration in vascular transplantation models (49). M3 has shown promise as an anti-inflammatory therapeutic in several models, including tumor rejection (50) and vascular injury (51). Islet-specific M3 expression can also prevent inflammatory recruitment, islet destruction, and subsequent diabetes in mouse insulitis models (52). The discovery of R17 as a novel chemokine decoy receptor with unique chemokine and GAG binding properties sets the stage for future experiments evaluating its therapeutic potential in similar experimental models.

REFERENCES

1. **Loh J, Zhao G, Nelson CA, Coder P, Droit L, Handley SA, Johnson LS, Vachharajani P, Guzman H, Tesh RB, Wang D, Fremont DH, Virgin HW.** 2011. Identification and sequencing of a novel rodent gammaherpesvirus that establishes acute and latent infection in laboratory mice. J. Virol. **85**:2642–2656. http://dx.doi.org/10.1128/JVI.01661-10.
2. **Virgin HW, IV, Latreille P, Wamsley P, Hallsworth K, Weck KE, Dal Canto AJ, Speck SH.** 1997. Complete sequence and genomic analysis of murine gammaherpesvirus 68. J. Virol. **71**:5894–5904.
3. **Russo JJ, Bohenzky RA, Chien MC, Chen J, Yan M, Maddalena D, Parry JP, Peruzzi D, Edelman IS, Chang Y, Moore PS.** 1996. Nucleotide sequence of the Kaposi sarcoma-associated herpesvirus (HHV8). Proc. Natl. Acad. Sci. U. S. A. **93**:14862–14867. http://dx.doi.org/10.1073/pnas.93.25.14862.
4. **Herr RA, Wang X, Loh J, Virgin HW, Hansen TH.** 2012. Newly discovered viral E3 ligase pK3 induces endoplasmic reticulum-associated degradation of class I major histocompatibility proteins and their membrane-bound chaperones. J. Biol. Chem. **287**:14467–14479. http://dx.doi.org/10.1074/jbc.M111.325340.
5. **Alcami A, Koszinowski UH.** 2000. Viral mechanisms of immune evasion. Immunol. Today **21**:447–455. http://dx.doi.org/10.1016/S0167-5699(00)01699-6.
6. **Seet BT, Johnston JB, Brunetti CR, Barrett JW, Everett H, Cameron C, Sypula J, Nazarian SH, Lucas A, McFadden G.** 2003. Poxviruses and immune evasion. Annu. Rev. Immunol. **21**:377–423. http://dx.doi.org/10.1146/annurev.immunol.21.120601.141049.
7. **Murphy PM.** 2001. Viral exploitation and subversion of the immune system through chemokine mimicry. Nat. Immunol. **2**:116–122. http://dx.doi.org/10.1038/84214.
8. **Epperson ML, Lee CA, Fremont DH.** 2012. Subversion of cytokine networks by virally encoded decoy receptors. Immunol. Rev. **250**:199–215. http://dx.doi.org/10.1111/imr.12009.
9. **Alcami A, Lira SA.** 2010. Modulation of chemokine activity by viruses. Curr. Opin. Immunol. **22**:482–487. http://dx.doi.org/10.1016/j.coi.2010.06.004.
10. **Alcami A, Smith GL.** 1995. Vaccinia, cowpox, and camelpox viruses encode soluble gamma interferon receptors with novel broad species specificity. J. Virol. **69**:4633–4639.
11. **Alcami A, Smith GL.** 2002. The vaccinia virus soluble interferon-gamma receptor is a homodimer. J. Gen. Virol. **83**:545–549.
12. **Strockbine LD, Cohen JI, Farrah T, Lyman SD, Wagener F, DuBose RF, Armitage RJ, Spriggs MK.** 1998. The Epstein-Barr virus BARF1 gene encodes a novel, soluble colony-stimulating factor-1 receptor. J. Virol. **72**:4015–4021.
13. **Lau EK, Allen S, Hsu AR, Handel TM.** 2004. Chemokine-receptor interactions: GPCRs, glycosaminoglycans and viral chemokine binding proteins. Adv. Protein Chem. **68**:351–391. http://dx.doi.org/10.1016/S0065-3233(04)68010-7.
14. **Alexander JM, Nelson CA, van Berkel V, Lau EK, Studts JM, Brett TJ, Speck SH, Handel TM, Virgin HW, Fremont DH.** 2002. Structural basis of chemokine sequestration by a herpesvirus decoy receptor. Cell **111**:343–356. http://dx.doi.org/10.1016/S0092-8674(02)01007-3.
15. **Alexander-Brett JM, Fremont DH.** 2007. Dual GPCR and GAG mimicry by the M3 chemokine decoy receptor. J. Exp. Med. **204**:3157–3172. http://dx.doi.org/10.1084/jem.20071677.
16. **Wang D, Bresnahan W, Shenk T.** 2004. Human cytomegalovirus encodes a highly specific RANTES decoy receptor. Proc. Natl. Acad. Sci. U. S. A. **101**:16642–16647. http://dx.doi.org/10.1073/pnas.0407233101.
17. **Viejo-Borbolla A, Martinez-Martin N, Nel HJ, Rueda P, Martin R, Blanco S, Arenzana-Seisdedos F, Thelen M, Fallon PG, Alcami A.** 2012. Enhancement of chemokine function as an immunomodulatory strategy employed by human herpesviruses. PLoS Pathog. **8**:e1002497. http://dx.doi.org/10.1371/journal.ppat.1002497.
18. **Graham KA, Lalani AS, Macen JL, Ness TL, Barry M, Liu LY, Lucas A, Clark-Lewis I, Moyer RW, McFadden G.** 1997. The T1/35kDa family of poxvirus-secreted proteins bind chemokines and modulate leukocyte influx into virus-infected tissues. Virology **229**:12–24. http://dx.doi.org/10.1006/viro.1996.8423.
19. **Alcami A, Symons JA, Collins PD, Williams TJ, Smith GL.** 1998. Blockade of chemokine activity by a soluble chemokine binding protein from vaccinia virus. J. Immunol. **160**:624–633.
20. **Arnold PL, Fremont DH.** 2006. Structural determinants of chemokine binding by an ectromelia virus-encoded decoy receptor. J. Virol. **80**:7439–7449. http://dx.doi.org/10.1128/JVI.00576-06.
21. **Lalani AS, Graham K, Mossman K, Rajarathnam K, Clark-Lewis I, Kelvin D, McFadden G.** 1997. The purified myxoma virus gamma interferon receptor homolog M-T7 interacts with the heparin-binding domains of chemokines. J. Virol. **71**:4356–4363.
22. **Bahar MW, Kenyon JC, Putz MM, Abrescia NG, Pease JE, Wise EL, Stuart DI, Smith GL, Grimes JM.** 2008. Structure and function of A41, a vaccinia virus chemokine binding protein. PLoS Pathog. **4**:e5. http://dx.doi.org/10.1371/journal.ppat.0040005.
23. **Ruiz-Arguello MB, Smith VP, Campanella GS, Baleux F, Arenzana-Seisdedos F, Luster AD, Alcami A.** 2008. An ectromelia virus protein that interacts with chemokines through their glycosaminoglycan binding domain. J. Virol. **82**:917–926. http://dx.doi.org/10.1128/JVI.02111-07.
24. **Alejo A, Ruiz-Arguello MB, Ho Y, Smith VP, Saraiva M, Alcami A.** 2006. A chemokine-binding domain in the tumor necrosis factor receptor from variola (smallpox) virus. Proc. Natl. Acad. Sci. U. S. A. **103**:5995–6000. http://dx.doi.org/10.1073/pnas.0510462103.
25. **Lalani AS, Masters J, Graham K, Liu L, Lucas A, McFadden G.** 1999. Role of the myxoma virus soluble CC-chemokine inhibitor glycoprotein, M-T1, during myxoma virus pathogenesis. Virology **256**:233–245. http://dx.doi.org/10.1006/viro.1999.9617.
26. **Lateef Z, Baird MA, Wise LM, Mercer AA, Fleming SB.** 2009. Orf virus-encoded chemokine-binding protein is a potent inhibitor of inflammatory monocyte recruitment in a mouse skin model. J. Gen. Virol. **90**:1477–1482. http://dx.doi.org/10.1099/vir.0.009589-0.
27. **Lateef Z, Baird MA, Wise LM, Young S, Mercer AA, Fleming SB.** 2010. The chemokine-binding protein encoded by the poxvirus ORF virus inhibits recruitment of dendritic cells to sites of skin inflammation and migration to peripheral lymph nodes. Cell. Microbiol. **12**:665–676. http://dx.doi.org/10.1111/j.1462-5822.2009.01425.x.
28. **van Berkel V, Levine B, Kapadia SB, Goldman JE, Speck SH, Virgin HW, IV.** 2002. Critical role for a high-affinity chemokine-binding protein in gamma-herpesvirus-induced lethal meningitis. J. Clin. Invest. **109**:905–914. http://dx.doi.org/10.1172/JCI14358.
29. **Hughes DJ, Kipar A, Sample JT, Stewart JP.** 2010. Pathogenesis of a model gammaherpesvirus in a natural host. J. Virol. **84**:3949–3961. http://dx.doi.org/10.1128/JVI.02085-09.
30. **Hughes DJ, Kipar A, Leeming GH, Bennett E, Howarth D, Cummerson JA, Papoula-Pereira R, Flanagan BF, Sample JT, Stewart JP.** 2011. Chemokine binding protein M3 of murine gammaherpesvirus 68 modulates the host response to infection in a natural host. PLoS Pathog. **7**:e1001321. http://dx.doi.org/10.1371/journal.ppat.1001321.
31. **Proudfoot AE, Borlat F.** 2000. Purification of recombinant chemokines from E. coli. Methods Mol. Biol. **138**:75–87.
32. **Miley MJ, Truscott SM, Yu YY, Gilfillan S, Fremont DH, Hansen TH, Lybarger L.** 2003. Biochemical features of the MHC-related protein 1 consistent with an immunological function. J. Immunol. **170**:6090–6098.
33. **Kelley LA, Sternberg MJ.** 2009. Protein structure prediction on the Web: a case study using the Phyre server. Nat. Protoc. **4**:363–371. http://dx.doi.org/10.1038/nprot.2009.2.

34. **Houser B.** 2012. Bio-Rad's Bio-Plex(R) suspension array system, xMAP technology overview. Arch. Physiol. Biochem. **118:**192–196. http://dx.doi .org/10.3109/13813455.2012.705301.

35. **Cyster JG.** 1999. Chemokines and cell migration in secondary lymphoid organs. Science **286:**2098–2102. http://dx.doi.org/10.1126/science.286 .5447.2098.

36. **Moser B, Loetscher P.** 2001. Lymphocyte traffic control by chemokines. Nat. Immunol. **2:**123–128. http://dx.doi.org/10.1038/84219.

37. **Jensen KK, Chen SC, Hipkin RW, Wiekowski MT, Schwarz MA, Chou CC, Simas JP, Alcami A, Lira SA.** 2003. Disruption of CCL21-induced chemotaxis in vitro and in vivo by M3, a chemokine-binding protein encoded by murine gammaherpesvirus 68. J. Virol. **77:**624–630. http://dx .doi.org/10.1128/JVI.77.1.624-630.2003.

38. **Maghazachi AA.** 2000. Intracellular signaling events at the leading edge of migrating cells. Int. J. Biochem. Cell Biol. **32:**931–943. http://dx.doi.org /10.1016/S1357-2725(00)00035-2.

39. **van Berkel V, Barrett J, Tiffany HL, Fremont DH, Murphy PM, McFadden G, Speck SH, Virgin HI.** 2000. Identification of a gammaherpesvirus selective chemokine binding protein that inhibits chemokine action. J. Virol. **74:**6741–6747. http://dx.doi.org/10.1128/JVI.74.15.6741-6747 .2000.

40. **Proudfoot AE, Handel TM, Johnson Z, Lau EK, LiWang P, Clark-Lewis I, Borlat F, Wells TN, Kosco-Vilbois MH.** 2003. Glycosaminoglycan binding and oligomerization are essential for the in vivo activity of certain chemokines. Proc. Natl. Acad. Sci. U. S. A. **100:**1885–1890. http://dx.doi .org/10.1073/pnas.0334864100.

41. **Esko JD, Weinke JL, Taylor WH, Ekborg G, Roden L, Anantharamaiah G, Gawish A.** 1987. Inhibition of chondroitin and heparan sulfate biosynthesis in Chinese hamster ovary cell mutants defective in galactosyltransferase I. J. Biol. Chem. **262:**12189–12195.

42. **Cardin AD, Weintraub HJ.** 1989. Molecular modeling of protein-glycosaminoglycan interactions. Arteriosclerosis **9:**21–32. http://dx.doi .org/10.1161/01.ATV.9.1.21.

43. **Hileman RE, Fromm JR, Weiler JM, Linhardt RJ.** 1998. Glycosaminoglycan-protein interactions: definition of consensus sites in glycosaminoglycan binding proteins. Bioessays **20:**156–167. http://dx.doi.org/10 .1002/(SICI)1521-1878(199802)20:2<156::AID-BIES8>3.0.CO;2-R.

44. **Lau EK, Paavola CD, Johnson Z, Gaudry JP, Geretti E, Borlat F, Kungl AJ, Proudfoot AE, Handel TM.** 2004. Identification of the glycosaminoglycan binding site of the CC chemokine, MCP-1: implications for structure and function in vivo. J. Biol. Chem. **279:**22294–22305. http://dx.doi .org/10.1074/jbc.M311224200.

45. **Seet BT, Barrett J, Robichaud J, Shilton B, Singh R, McFadden G.** 2001. Glycosaminoglycan binding properties of the myxoma virus CC-chemokine inhibitor, M-T1. J. Biol. Chem. **276:**30504–30513. http://dx .doi.org/10.1074/jbc.M011401200.

46. **Lucas A, McFadden G.** 2004. Secreted immunomodulatory viral proteins as novel biotherapeutics. J. Immunol. **173:**4765–4774.

47. **Dabbagh K, Xiao Y, Smith C, Stepick-Biek P, Kim SG, Lamm WJ, Liggitt DH, Lewis DB.** 2000. Local blockade of allergic airway hyperreactivity and inflammation by the poxvirus-derived pan-CC-chemokine inhibitor vCCI. J. Immunol. **165:**3418–3422.

48. **Bursill CA, Cai S, Channon KM, Greaves DR.** 2003. Adenoviral-mediated delivery of a viral chemokine binding protein blocks CC-chemokine activity in vitro and in vivo. Immunobiology **207:**187–196. http://dx.doi.org/10.1078/0171-2985-00228.

49. **Liu L, Dai E, Miller L, Seet B, Lalani A, Macauley C, Li X, Virgin HW, Bunce C, Turner P, Moyer R, McFadden G, Lucas A.** 2004. Viral chemokine-binding proteins inhibit inflammatory responses and aortic allograft transplant vasculopathy in rat models. Transplantation **77:**1652–1660. http://dx.doi.org/10.1097/01.TP.0000131173.52424.84.

50. **Rice J, de Lima B, Stevenson FK, Stevenson PG.** 2002. A gamma-herpesvirus immune evasion gene allows tumor cells in vivo to escape attack by cytotoxic T cells specific for a tumor epitope. Eur. J. Immunol. **32:**3481–3487. http://dx.doi.org/10.1002/1521-4141(200212)32:12<3481::AID -IMMU3481>3.0.CO;2-J.

51. **Pyo R, Jensen KK, Wiekowski MT, Manfra D, Alcami A, Taubman MB, Lira SA.** 2004. Inhibition of intimal hyperplasia in transgenic mice conditionally expressing the chemokine-binding protein M3. Am. J. Pathol. **164:**2289–2297. http://dx.doi.org/10.1016/S0002-9440(10)63785-6.

52. **Martin AP, Canasto-Chibuque C, Shang L, Rollins BJ, Lira SA.** 2006. The chemokine decoy receptor M3 blocks CC chemokine ligand 2 and CXC chemokine ligand 13 function in vivo. J. Immunol. **177:**7296–7302.